Available online at www.sciencedirect.com

SCIENCE DIRECT®

Developmental Biology 271 (2004) 322–338

DEVELOPMENTAL BIOLOGY

www.elsevier.com/locate/ydbio

Proximo-distal specialization of epithelial transport processes within the *Xenopus* pronephric kidney tubules☆

Xiaolan Zhou and Peter D. Vize*

Department of Biological Science, University of Calgary, Calgary, Alberta, Canada T2N 1N4
Department of Biochemistry and Molecular Biology, University of Calgary, Calgary, Alberta, Canada T2N 1N4

Received for publication 11 December 2003, revised 20 February 2004, accepted 22 March 2004
Available online 13 May 2004

Abstract

The embryonic kidneys of larval aquatic vertebrates such as fish and frogs serve as excellent model systems for exploring the early development of nephric organs. These experimental systems can easily be manipulated by microsurgery, microinjection, genetics, or combinations of these approaches. However, little is known about how physiologically similar these simple kidneys are to the more complex mammalian adult kidneys. In addition, almost nothing is known about proximo-distal patterning of nephrons in any organism. In order begin to explore the physiological specialization of the pronephric tubules along the proximo-distal axis, a combination of uptake assays using fluorescently tagged proteins, LDL particles and dextrans, and an informatics-targeted in situ screen for transport proteins have been performed on embryos of the frog, *Xenopus laevis*. Genes identified to be expressed within unique subdomains of the pronephric tubules include an ABC transporter, two amino acid cotransporters, two sodium bicarbonate cotransporters, a novel sodium glucose cotransporter, a sodium potassium chloride cotransporter (NKCC2), a sodium chloride organic solute cotransporter (ROSIT), and a zinc transporter. A novel combination of colorimetric and fluorescent whole-mount in situ hybridization (FCIS) was used to precisely map the expression domain of each gene within the pronephros. These data indicate specialized physiological function and define multiple novel segments of the pronephric tubules, which contain at least six distinct transport domains. Uptake studies identified functional transport domains and also demonstrated that early glomeral leakage can allow visualization of protein movement into the pronephric tubules and thus establish a system for investigating experimentally induced proteinuria and glomerulonephritis.

Keywords: Pronephros; Bartter's syndrome; Transporter; Cotransporter; ROSIT; NKCC2; NBC; SGLT; SLC3; SLC4; SLC5; SLC6; SLC7; SLC30; Malabsorption

Introduction

Vertebrates that live in a fresh water environment must constantly excrete large volumes of dilute urine to cope with the constant influx of water through the skin and gut (Vize et al., 2003b). Ions are in low concentrations in such environments and fresh water vertebrates expend much energy using active transport processes to take up ions from the surrounding medium. This combination of circumstances—the need to produce large volumes of urine and the need to minimize ion loss—means that embryonic kidneys must be extremely efficient at resorptive processes. Molecules that must be effectively recovered from the kidney filtrate include inorganic and organic ions, amino acids, bicarbonate, carbohydrates, lipids, and sometimes water itself (Dantzler, 1988).

Amphibian kidneys, both embryonic and adult, function by the same filtration–resorption processes that functions in mammals. In fact, this process was first discovered in micropuncture studies of amphibian kidneys by Richards and colleagues (reviewed by Richards, 1929). There are however some differences between these various kidneys. For example, aquatic amphibians excrete nitrogen as ammonia, not urea, and only switch to production of urea following metamorphosis and the move to a terrestrial habitat (Balinsky, 1970; Vize et al., 2003a). Ammonia, while toxic, is not a problem in aquatic animals due to the dilute nature and large volumes of urine. Another important difference is the method by which the kidney filtrate is supplied to the kidney tubules.

☆ Supplementary data for this article are available on Science Direct.

* Corresponding author. Department of Biological Science, University of Calgary, 2500 University Drive NW, Calgary, Alberta Canada T2N 1N4. Fax: +403-289-9311.
E-mail address: pvize@ucalgary.ca (P.D. Vize).

0012-1606/$ - see front matter © 2004 Elsevier Inc. All rights reserved.
doi:10.1016/j.ydbio.2004.03.036

In adult kidneys, hydrostatic pressure drives filtration through the glomerulus and directly into the associated nephron. In embryonic pronephric kidneys, the glomus delivers waste to the body cavity, or coelom (Goodrich, 1930). Fluids in the coelom are swept into the pronephric tubules through thin funnels called nephrostomes that are lined with hundreds of cilia, and ciliary motion drives fluid transport (Fox, 1963). Once the filtrate has been produced and swept into the pronephric tubules, useful molecules are resorbed. Pronephric proximal tubules contain lipid inclusions that indicate recovery of lipids and cholesterol from the filtrate (Gérard and Cordier, 1934a,b).

A key player in driving transport of small molecules and ions across the kidney epithelial membranes is the sodium potassium ATPase. This transporter generates low sodium and high potassium concentrations in the kidney epithelium, and these in turn power a variety of cotransporters that utilize the resulting electrochemical gradient to resorb useful molecules from the kidney filtrate. The high level expression of Na^+K^+ATPases in the pronephric tubules has been described in some reports including Drummond et al. (1998a,b), Eid and Brandli (2001), and Uochi et al. (1997). In the present report, the expression of some of the genes whose protein products utilize cotransport with sodium ions is examined, with the Na^+K^+-ATPase being used as a general pronephric marker for comparative purposes.

In addition to Na^+K^+ATPases, two other proteins that may function in pronephric epithelial transport have recently been described, an SGLT transporter (Eid et al., 2002; Nagata et al., 1999) and a chloride conductance channel (Vize, 2003). In this report, nine novel transporter proteins are added to this group. In many cases, the expression of these new genes occurs in segments of the pronephros that have not previously been identified to have specialized physiological function. Examples of transporters limited to early or late subdomains of both the proximal or distal tubule are described, indicating that the pronephric tubules share a segmental complexity comparable to that of mammalian nephrons. Furthermore, we directly measure the uptake of fluorescently labeled carbohydrates, proteins, and lipids within the proximal tubule segment of the pronephroi. The introduction of fluorescently tagged macromolecules into the tadpole circulatory system results in filtration into the nephrons in 54–95% of pronephroi. This generates fluorescent urine and allows the simple visualization of resorption across the pronephric epithelium.

The degree of physiological complexity demonstrated by these data indicates that as predicted, amphibian pronephroi are extremely complex organs performing a myriad of balanced transport processes to maintain internal solute and pH levels in a challenging environment. Given the experimental manipulability of the frog embryonic kidney, this system may be extremely useful in investigating developmental processes that generate the complex segregation of various transport systems to distinct segments of the nephron.

Methods

Embryos

Standard *Xenopus laevis* husbandry techniques were used to generate and raise embryos (Sive et al., 2000).

Renal uptake assays

Alexa 488-conjugated acetylated LDL (Levine et al., 2003), Texas Red-conjugated serum albumin (66 kDa), Alexa 488-conjugated codfish parvalbumin (12.3 kDa), 70 and 500 kDa FITC tagged dextran were all from Molecular Probes and 160 kDa TRITC dextran was from Sigma. These reagents were dissolved to a concentration of 50 mg/ml in sterile water. Approximately, 7 nl of solution was injected (two pulses of 3.5 nl) into the beating hearts of benzocaine anesthetized *X. laevis* tadpoles at stage 38–42. The distribution of the fluor was monitored by fluorescence stereomicroscopy (Leica FLZIII) for up to 4 h.

In situ hybridization

Clones encoding transporters from the IMAGE consortium were obtained from OpenBiosystems. The IMAGE numbers were XABC1, 4032165; XAA1, 4030633; XAA2, 4930123; XROSIT, 4032864; XNBC1, 4032876; XNBC2, 4032091; XSGLT1K, 4959902; XNKCC2, 4033317; XZnSLC30, 5537474, and the Na^+K^+ATPase alpha-1 subunit 4030702. All of these clones were cut with *Sma*I and transcribed with T7 to generate antisense digoxygenin labeled probes for in situ hybridization, except for XAA1 that has an internal *Sma*I site, so *Eco*RV was used for linearization. Standard colorimetric in situ methods were utilized (Harland, 1991). Fluorescent whole-mount in situs (FISH) were performed using tyramide-FITC (Davidson and Keller, 1999) or tyramide-Cy3. Tyramide-Cy3 was generated using Cy3 mono NHS ester (Amersham PA13101) and tyramide (Sigma T-2879). A 10 mg/ml stock of Cy3-NHS ester was made in dimethylformamide (DMF). This solution (100 μl) was then mixed with 33 μl of 10 mg/ml tyramide in 100:1 (v/v) DMF/triethylamide and incubated at room temperature for 2 h. Ethanol (1.2 ml) was then added and the Cy3-tyramide stored at −20 °C. The tyramide was used at a final concentration of 1/100 in phosphate-buffered saline for horseradish-peroxidase (HRP)-driven development.

FCIS

A novel combination of fluorescent and colorimetric in situ (FCIS) was also employed. This was performed using a

combination of digoxygenin-labeled RNA probes for test genes and an FITC-labeled RNA probe for the general pronephric marker Na^+K^+ATPase. Both probes were hybridized simultaneously, and both detected with simultaneous incubation with appropriate antibodies. The transporter was detected using an alkaline-phosphatase (AP) coupled anti-digoxygenin antibody and developing using BM purple substrate (Roche) or NBT/BCIP. The counterstain was detected with an HRP-coupled anti-FITC antibody (Roche) and developed using an FITC- or Cy3-tyramide substrate. In brief, this was done by rinsing in phosphate-buffered saline plus 0.1% Tween-20 (PBST) then incubating in PBST plus FITC-tyramide (1/100) for 20 min. H_2O_2 was then added to 0.001% (v/v) and the reaction incubated at room temperature for 30 min. Washing was then performed in multiple changes of tris-buffered saline for 20–24 h to remove unreacted tyramide. The purple AP substrate was then developed, embryos post-fixed and bleached in 70% methanol/10% H_2O_2, then photographed. A detailed protocol is available at http://xenbase.org/methods.

The overlay of bright-field images of the purple reaction product and the fluorescent tyramide product was performed using Photoshop 7 (Adobe). This process is somewhat convoluted and so is outlined in brief. The FITC fluorescent image is copied (Select All) and pasted into the red channel of a new Photoshop document window of equal dimensions. The green channel of the new document is filled with black. The bright-field image is opened separately and desaturated. This is then converted to gray scale, copied, and pasted into the green channel of the new document. It is also pasted into the blue channel, which is then inverted. Brightness and contrast can be modified in individual channels to enhance the final image. Strong staining will appear as blue, overlap as pink, and FITC only as orange. For a simple composite image, the two images can be pasted into different layers and the opacity slider used to generate a hybrid.

Results

Pronephric tubule domain nomenclature

The expression of transporter genes discussed below occurs in some hitherto unidentified subdomains, or segments, of the pronephric tubules. To simplify the description of these segments, Fig. 1 illustrates the nomenclature that has been adopted. This nomenclature is based up that previously used to describe amphibian mesonephric nephrons, which have been subdivided into a single proximal domain, a short (only sometimes present) ciliated intermediate segment, an early distal segment, and a late distal segment (Biemesderfer et al., 1989; Møbjerg et al., 1998; Stanton et al., 1984; Yucha and Stoner, 1986). The early distal segment is sometimes called the diluting segment. The major subdivisions of mesonephric nephrons are consistent

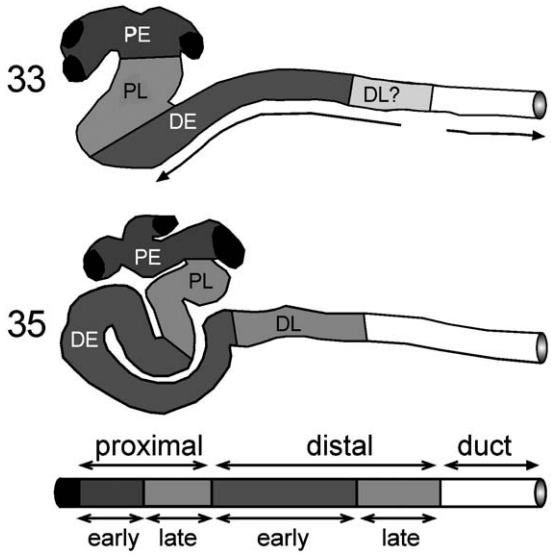

Fig. 1. Pronephric tubule segment nomenclature. Schematics of stage 33 and stage 35 pronephroi are presented with the borders between early and late segments within both proximal and distal domains marked with dark and light gray, respectively (see Møbjerg et al., 1998 for mesonephric nomenclature). The tips of the dorsal branches are colored black. In the stage 33, pronephros the presumptive late distal segment (DL?) is shown with a stippled pattern, this cannot be confirmed as no markers of the late distal segment expressed at this stage of development have been reported. As convergence and extension drives the pronephros posteriorly toward the cloaca, it also pushes the early and late distal segments anteriorly where they coil ventral to the proximal domain (see arrows). PE, proximal early. PL, proximal late. DE, distal early. DL, distal late. Duct, pronephric duct.

with histological studies of pronephric nephrons (Kluge and Fischer, 1991; Møbjerg et al., 2000), so were adopted to formulate the nomenclature used here. The present study also identified a subdivision of the proximal domain. To remain consistent with the distal segment nomenclature, these were named the early and late proximal segments.

The pronephric tubules are linked to the coelomic cavity via nephrostomes, thin ciliated tubules that are not visible in any of the patterns presented here. Nephrostomes are linked to the early proximal tubule segment by three dorsal branches, shown in black in Fig. 1. The early proximal domain corresponds to the region previously called the connective tubule (Vize et al., 1995) as it links the dorsal branches to the late proximal domain, the region previously called the broad or common tubule (Fox, 1963).

Renal uptake analysis

The ability of pronephroi to filter and resorb glucose polymers (dextrans), proteins, and acetylated LDL particles was measured by injecting fluorescently tagged macromolecules into the circulatory system of tadpoles, shortly after the onset of pronephric function at NF stage 37/38. Injections were performed by cardiac puncture, and within 10 min, fluor could be observed in the lumen of the pronephric tubules and pronephric duct, and fluorescent urine was observed flowing rapidly into the medium. The volume of

urine generated by tadpoles is extraordinary and is illustrated via real-time video that can be viewed in the supplemental materials (BSA_proteinuria.mov). Often, the pronephric system and the heart were the only labeled features obvious in injected embryos, although serum albumin and acetylated LDL also labeled endothelial cells at a lower frequency. Some embryos displayed fluorescence throughout the lumen of the pronephric system (e.g., Figs. 2B, C), while others displayed fluorescence only in the epithelia of the proximal tubules (Figs. 2E, F). In both instances, the fluor must cross the glomeral filtration barrier. The first form of pronephric labeling (lumenal) illustrates

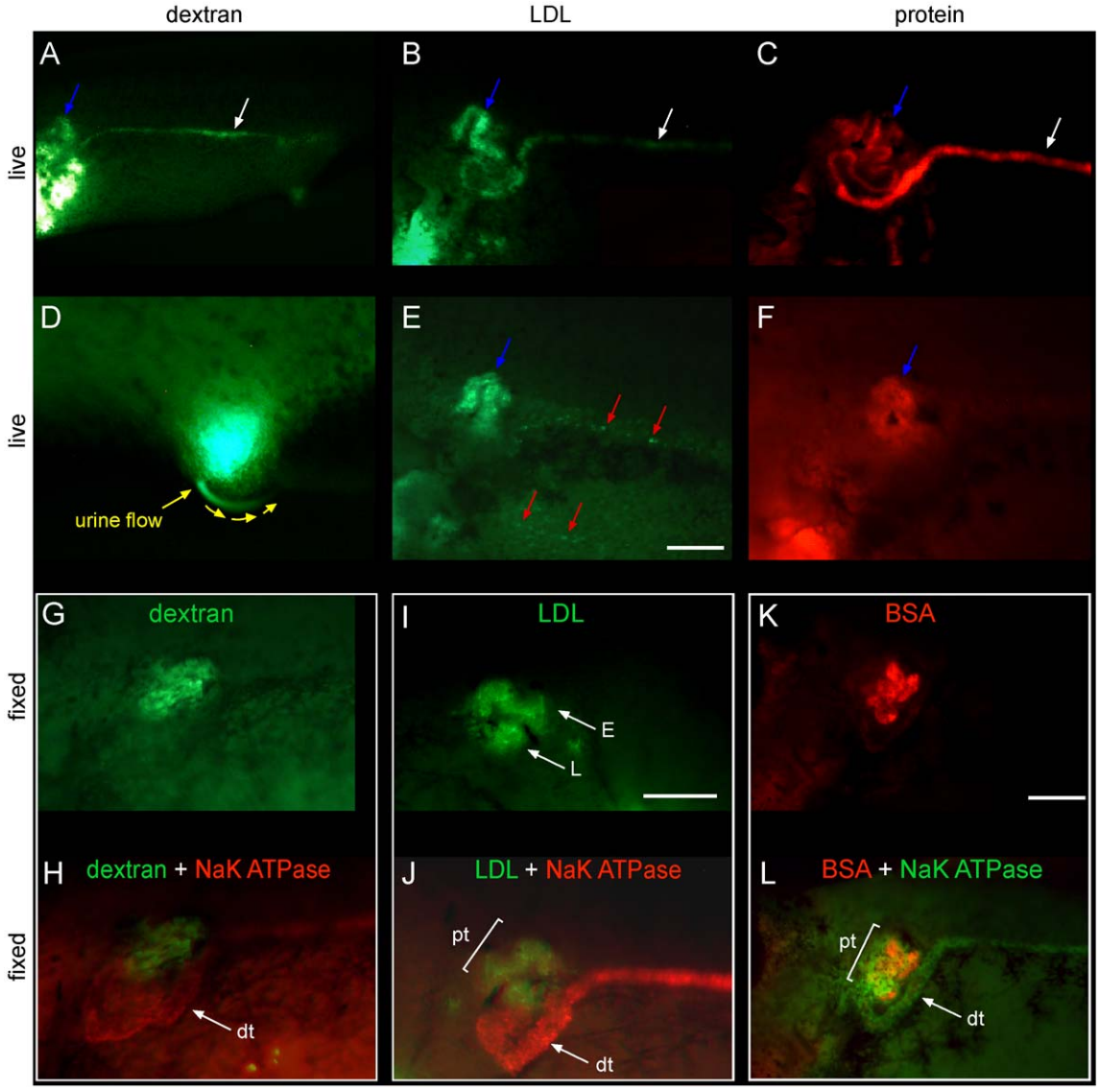

Fig. 2. Resorption of macromolecules by the proximal segment. The blood of embryos was labeled by cardiac injection of fluor-tagged dextrans, LDL particles, or proteins. Embryos were photographed 15 min post injection for live images, or allowed to resorb for 2–20 h then fixed and counterstained for Na^+K^+ATPase expression via FISH. (A) Dextrans cross the pronephric glomeral filtration barrier are excreted. Fluorescent 70 kDa dextran can be seen in the lumen of proximal tubules (blue arrow), distal tubule, and pronephric duct (white arrow) 15 min post injection in live embryo. (B) LDL particles cross the glomeral filtration barrier and are excreted. Fifteen minutes post injection, live embryo. Both the lumen and the epithelium of the proximal segment are fluorescent, while only the lumen of the distal segment and duct is labeled. (C) Serum albumin in the lumen of pronephric tubules 15 min post injection, live embryo. (D) Fluorescent urine (yellow arrow) from filtered 70 kDa dextran flowing from the cloaca. A real-time animation of protein excretion in urine is also available in the supplemental materials (BSA_proteinuria.mov). (E) Example of acetylated LDL resorption out-competing excretion. Little or no LDL is present in the lumen or urine. Red arrows indicate labeled endothelial cells. (F) Resorption of serum albumin by proximal tubules of a living tadpole. (G) Localization of 70 kDa FITC-dextran resorption, 20 h post injection. (H) Counterstain of "G" with Na^+K^+ATPase and a Cy3-tyramide substrate. Both FITC and Cy3 channels are shown. (I) Localization of Alexa488-LDL resorption domain. Tadpole was fixed 2 h post LDL injection. (J) Counterstain of "I" with Na^+K^+ATPase and a Cy3-tyramide substrate. Both Alexa-488 and Cy3 channels are shown. (K) Resorption of serum albumin. Tadpole was fixed 2 h post serum albumin injection. (L) Counterstain of the sample shown in "K" with Na^+K^+ATPase using an FITC-tyramide. The distal tubule (dt) has no serum albumin, nor does the duct. Both Texas Red (serum albumin) and FITC channels are shown. Scale bars represent 200 μm. Unlabeled blue arrows, proximal tubule. Unlabeled white arrows, pronephric duct. Unlabeled red arrows, endothelial cells.

Table 1
Excretion and resorption by pronephros

	Stage	MW	# Tadpoles	In urine	# Kidneys	% Kidneys
Dextran-TRITC	38	160 k	10	10	18	90
Dextran-FITC	40	500 k	11	11	21	95
Parvalbumin-Alexa488	38	12.3 k	12	11	20	91
Serum albumin-Texas Red	38	66 k	13	13	14	54
LDL-Alexa488	41	n/a	6	5	8	80

excretion, while the second (epithelial) documents filtration followed by resorption (Figs. 2E, F). By 1 h post injection, most of the injected fluor had been resorbed by pronephroi or cleared via excretion. Even large molecular weight dextrans and serum albumin were observed in the kidney lumen and were excreted in urine in many tadpoles, as were LDL particles and the low molecular weight protein parvalbumin. The frequency of excretion is lower with larger molecules (e.g., albumin vs. parvalbumin) and higher with dextrans than with proteins (Table 1).

Following injection of fluorescent macromolecules, approximately 20% of pronephroi have fluorescent proximal tubule epithelia after 15 min. This form of labeling is in the tubule epithelia, not the lumen (e.g., compare 2C to 2K), and represents epithelial recovery of the macromolecules, probably by endocytosis. This process is active in pronephroi for dextrans, LDL particles (or their labeled constituents), and proteins. Resorption of macromolecules by pronephric tubules is observed only in the proximal tubules—both early and late segments—and occurs in a gradient with highest levels at the most proximal and lowest levels near the border of the distal segment (Fig. 2E). Labeled tubules in living embryos (A–F) and in fixed embryos (G–L) counterstained for Na^+K^+ATPase expression are illustrated in Fig. 2.

These data demonstrate that macromolecule recovery processes are active in the proximal tubules of pronephroi. This may reflect active bulk endocytosis (Lencer et al., 1990) or may be mediated by more specific transport processes such as those that function in mammalian nephrons (for review, see Christensen and Birn, 2002), or a combination of the two.

Novel transporter gene identification

The *Xenopus* Gene Collection (http://xgc.nci.nih.gov/) includes an adult kidney cDNA library. Approximately 2500 sequences from this library were available in the NCBI EST database in early 2003 but were not annotated. An automated annotation of this sequence data using the MAGPIE system was kindly performed by Paul Gordon and Christoph Sensen (University of Calgary), and this analysis is publicly available at http://magpie.ucalgary.ca/magpie_xenopus.html. Level 1 matches were manually evaluated for potential usefulness based on the predicted physiological function. Particular focus was placed on transporter proteins that could potentially mediate processes active in early kidneys (Satlin et al., 2003). Forty-five clones that had the potential to function in early nephric physiological processes were identified and cDNAs obtained through IMAGE. The expression pattern of each of these genes was examined by whole-mount in situ hybridization of *Xenopus* embryos in the developmental window in which the pronephros forms and begins to form and function. Many clones showed either no expression in this window or general widespread transcription that failed to identify interesting expression within the kidney. Nine genes with strong pronephric expression patterns that indi-

Table 2
Novel pronephric transporter genes

Name	GenBank #	Closest match	% Ident (/) to species	Description
XABC	BU904610	BC044971	79% (243) to *Xenopus*	ATP-binding cassette, subfamily F (GCN20), member 2
		AAG13902	63% (248) to human	iron inhibited ABC transporter 2
XAA1	BU903271	BAA94300	64% (211) to mouse	B0 + amino acid transporter
		AAK43541	63% (211) to mouse	Na^+ and Cl^- coupled neutral and basic amino acid transporter
		NP_064433	63% (211) to mouse	Solute carrier family 6 (neurotransmitter transporter) member 14
XAA2	BC044971	AAH44971	90% (527) to *Xenopus*	Carrier family 7 (cationic amino acid transporter y+ system), #8
		NP_036376	80% (521) to human	solute carrier family 7 (cationic amino acid transp, y+ sys), #8
XSGLT1K	BM192615	CAC00574	62% (58) to human	Sodium/solute symporter family member similar to SLC5A1
		BAA22950.1	44% (58) to *Xenopus*	Na^+-glucose cotransporter type 1 (SGLT-1)-like
XNBC1	BU905206	AAB61339	74% (231) to salamander	Electrogenic Na^+ bicarbonate cotransporter
		AAC39840	74% (231) to human	Sodium bicarbonate cotransporter
XNBC2	BU904542	CAD55942	69% (231) to human	SLC-4, sodium bicarbonate transporter-like 1 (member 11)
XNKCC2	BU905556	Q13621	53% (174) to human	Kidney-specific Na-K-Cl symporter NKCC2
XROSIT	BU905195	AAC13771	54% (259) to rat	Renal osmotic stress-induced Na–Cl organic solute cotransport
XZnSLC30	BQ732178	AAH46675	91% (111) to *Xenopus*	Solute carrier family 30 (zinc transporter)
		NP_067017	67% (111) to human	Solute carrier family 30 (zinc transporter)

cated potential localized function were chosen for detailed analysis. Table 2 indicates the GenBank accession number for each of these clones, the closest related protein match identified by blastx, the closest mammalian protein match, and potential function. As some of these are not full-length protein alignments, the assignment of function is provisional, but the high degree of sequence conservation makes most of the annotations very likely to be correct. Genes that did not have expression that was strongly localized to the pronephroi are listed in the supplemental materials. The expression pattern of each gene was examined from stages in which the pronephric morphogenesis first begins (stage 24) up until the onset of pronephric function at stage 38/39 (Nieuwkoop and Faber, 1994). From within this data set, images that most clearly depict the spatial expression pattern were chosen and are described below. All images will be deposited at Xenbase (http://www.xenbase.org).

Sodium glucose cotransporter (SGLT, SLC5A)

Clone BM192615 (XSGLT1K) is most closely related to the large family (>220 members, Wright and Turk, 2004) of sodium glucose cotransporters (Table 2; Hediger et al., 1987). Tadpoles cannot afford to excrete glucose, and this transporter family plays a key role in resorption of a critical solute. Mutations in the closest human relative of XSGLT1K are responsible for glucose–galactose malabsorption syndrome (Martin et al., 1996). This particular transporter displays pronephric specific expression at very high levels and is therefore a useful marker for both in situ and RT-PCR analysis of kidney development. It is most closely related to human sodium glucose cotransporter SLC5A1 and is distinct (only 44% identical) from the *Xenopus* XSGT1L transporter previously described by Nagata et al. (1999), which is also expressed in the pro-

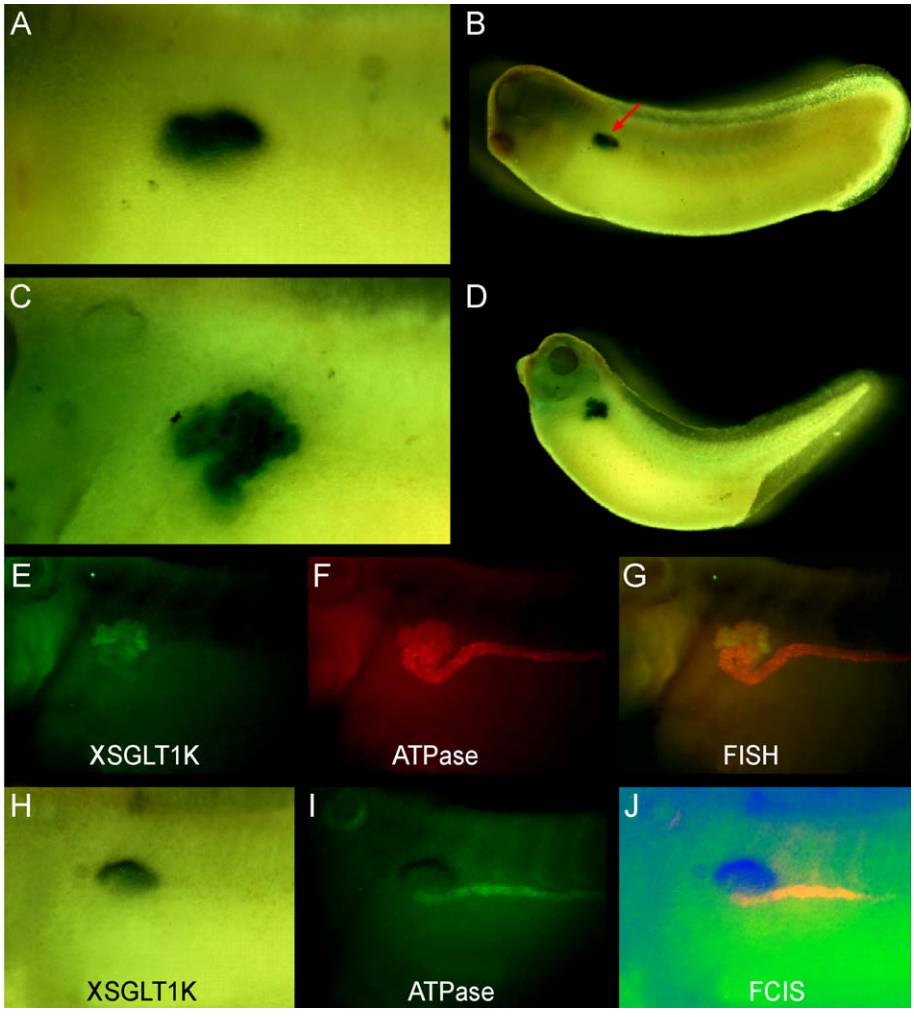

Fig. 3. Expression of XSGLT1k examined by colorimetric in situ, FISH and FCIS methodologies. (A and B) XSGLT1k expression in stage 28/29 pronephros (red arrow). (C and D) XSGLT1k expression in stage 37 pronephros. (E) XSGLT1K expression in stage 37 embryo detected via FISH with an FITC-tyramide substrate. (F) Na^+K^+ATPase expression in the same embryo as panel F, detected with a Cy3-tyramide substrate. (G) Overlay of panels E and F. The proximal domain expressing XSGLT1k appears green. (H) XSGLT1k expression in a stage 30 embryo developed with a purple substrate. (I) The same embryo as shown in panel H but developed for Na^+K^+ATPase expression with an FITC-tyramide substrate. (J) FCIS overlay of panels H and I performed via the protocol described in Methods. The XSGLT1k domain appears blue, while the pronephric tubules in which it is not expressed appear orange.

nephros (Eid et al., 2002). Both XSGLT1K and XSGLT1L are sodium glucose cotransporters (Hediger et al., 1987) and distinct from the facilitative sugar transporters such as GLUT and HMIT (reviewed by Wood and Trayhurn, 2003).

The expression pattern of XSGLT1K was also examined through a combination of double FISH and FCIS (Fig. 3). FCIS is an alternative to FISH that is particularly useful for genes expressed at low levels in small domains. The substrate development step of fluorescent in situ hybridization is more difficult to control as the reaction cannot be visualized and stopped at the optimal point, while colorimetric development allows fine control over signal intensity and signal to noise ratios. FCIS utilizes a standard purple or NBT/BCIP colorimetric development protocol coupled with a fluorescent in situ counterstain. The purple reaction product can be visualized either by bright-field microscopy or by fluorescence masking, as the precipitate blocks fluorescence of the counterstain. FCIS is performed by hybridizing two probes simultaneously, one labeled with digoxygenin (test gene) and one labeled with FITC (counterstain). Both probes are reacted with antihapten antibodies simultaneously, an alkaline phosphatase-coupled anti-digoxygenin antibody for the test gene, and an HRP-coupled anti-FITC antibody for the counterstain. The counterstain is developed first using a tyramide substrate as described in Methods, then washed and developed in purple substrate for the test gene. The Na^+K^+ATPase alpha subunit was used as a counterstain in both FISH and FCIS, as this gene is expressed at high levels throughout the developing pronephros (Drummond et al., 1998a,b).

XSGLT1K is expressed within both early and late proximal domains from stage 28 onwards (Fig. 3). Expression stops abruptly at the border between the late proximal and early distal segments, the same proximo-distal border respected by the 3G8 antigen (Vize et al., 1995).

Amino acid transporters (SLC6A14, SLC7A8)

The expression of two different amino acid transporters was examined, both of which have unique and very localized expression patterns. XAA1 is most closely related to SLC6A14, Na^+ and Cl^- coupled neutral and basic amino acid transporters that facilitate uptake of a broad spectrum of amino acids (Kekuda et al., 1996). In *Xenopus* embryos, XAA1 is expressed only in the late proximal segment of the pronephric tubules and is the first gene reported to be a

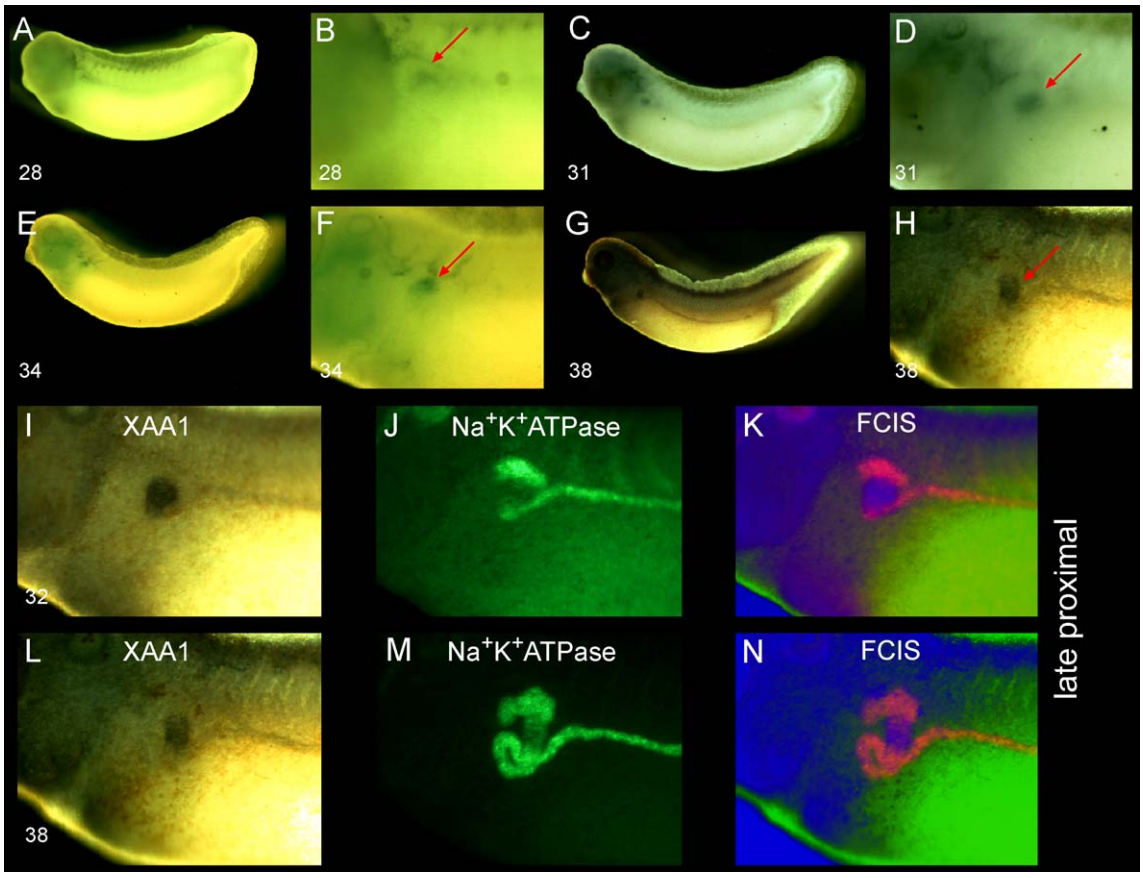

Fig. 4. Localization of XAA1 expression. Embryo stages are shown on the lower left of each panel. Panels A–H illustrate colorimetric in situs, and panels K and N FCIS with a Na^+K^+ATPase counterstain. XAA1 is strongly expressed in the late proximal segment from stages 32 onwards. Very low-level expression is also observed in the distal tubule and pronephric duct at stage 38.

marker of this domain (Fig. 4). Expression begins at stage 28. When single colorimetric in situs are performed for this gene, it appears as a small dot that cannot be accurately identified. FCIS clearly shows that expression is tightly restricted to only the late proximal domain.

XAA2 is related to SLC family 7 member 8, cationic amino acid transporters described by Torrents et al. (1998). It is expressed at high levels in the early proximal domain and at lower levels in the late proximal domain, with the onset of pronephric expression in the late domain occurring at NF stage 32 (Fig. 5). This pattern is maintained between stages 32 and 38, when the pronephric kidney becomes functional. The low-level expression in the late proximal segment (Fig. 1) can be also be seen as a masking of Na^+K^+ATPase fluorescence in the center panel, and is obvious in the multichannel overlay as a pink region (Fig. 5).

The proximal tubule is the major site of amino acid resorption in mammals (Silbernagl, 1988), consistent with the localized expression of XAA1 and XAA2.

ABC transporter

The ATP dependent family of ABC transporters encompasses an extremely broad group of membrane pumps with

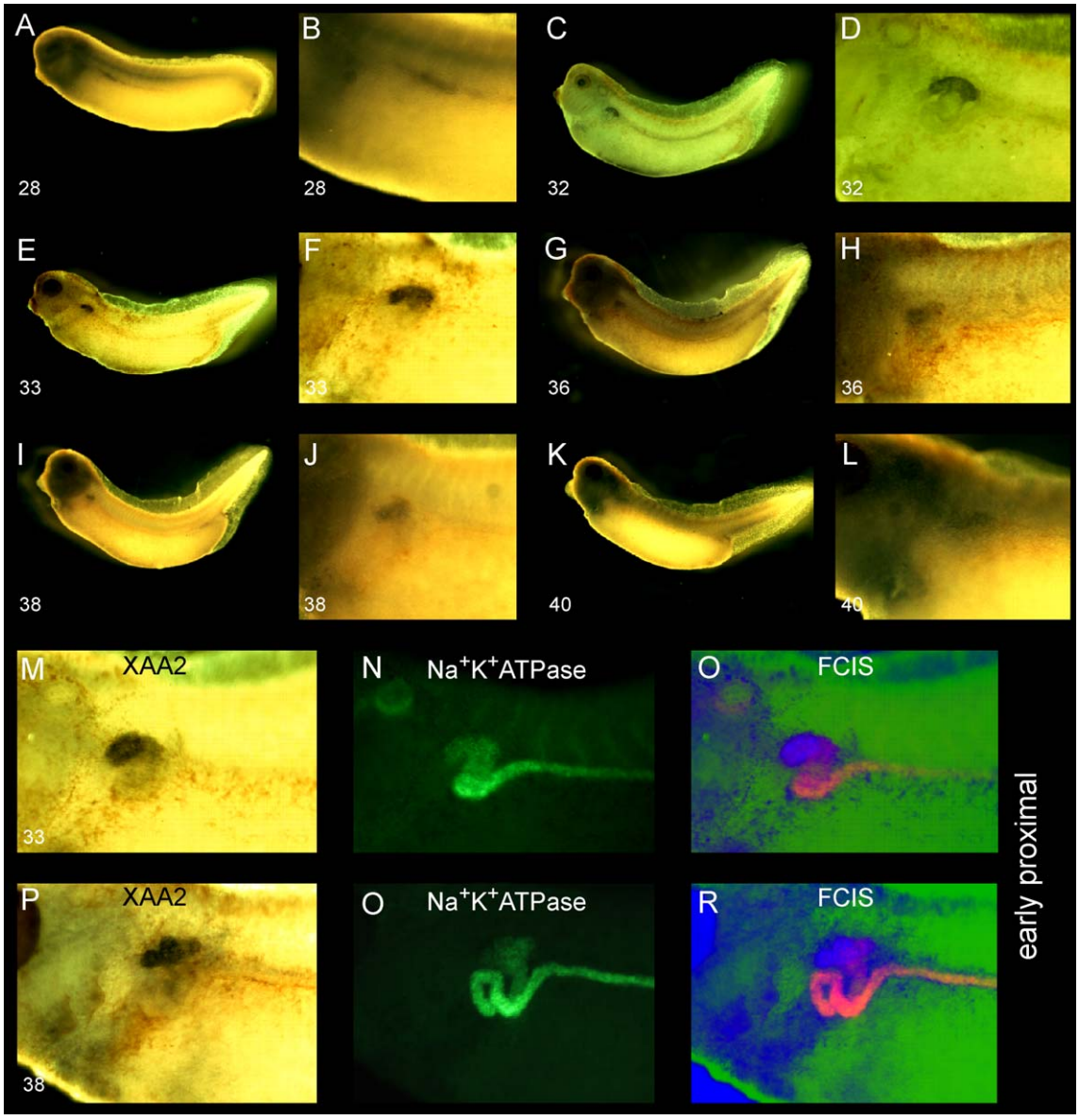

Fig. 5. XAA2 expression in the early proximal segment. In stage 28 embryos, low-level expression of XAA2 is observed in the future distal segment. This expression declines and is not detectable by stage 32. At stage 32, strong expression is activated in the early proximal tubule (C, D) and remains restricted to this segment until at least stage 40. Embryonic stages are shown at the lower left of panels A–L, M and P. The blue pronephric region in the FCIS panels shows the site of high level expression.

diverse functions. XABC1 encodes a member of this family with its closest match (Table 2) being to the human iron inhibited ABC transporter 2 (Ye and Connor, 2000).

XABC1 is expressed in the pronephric proximal tubule (Fig. 6) from stage 26. It is also expressed within other tissues near the pronephros, such as the somites and branchial arches. It is expressed in both early and late proximal pronephric segments. It is easiest to view XABC expression in earlier stages before the onset of expression in the somites.

Sodium bicarbonate cotransporters (NBC, SLC4A4, SLC4A11)

Bicarbonate must be transported across membranes to recover bicarbonate reserves from the kidney filtrate, to regulate pH, and to achieve balanced CO_2 metabolism (DuBose, 1990). When acid is produced in the distal segment for excretion, the bicarbonate generated in its production must also be recovered by the circulatory system. Two different sodium bicarbonate cotransporters

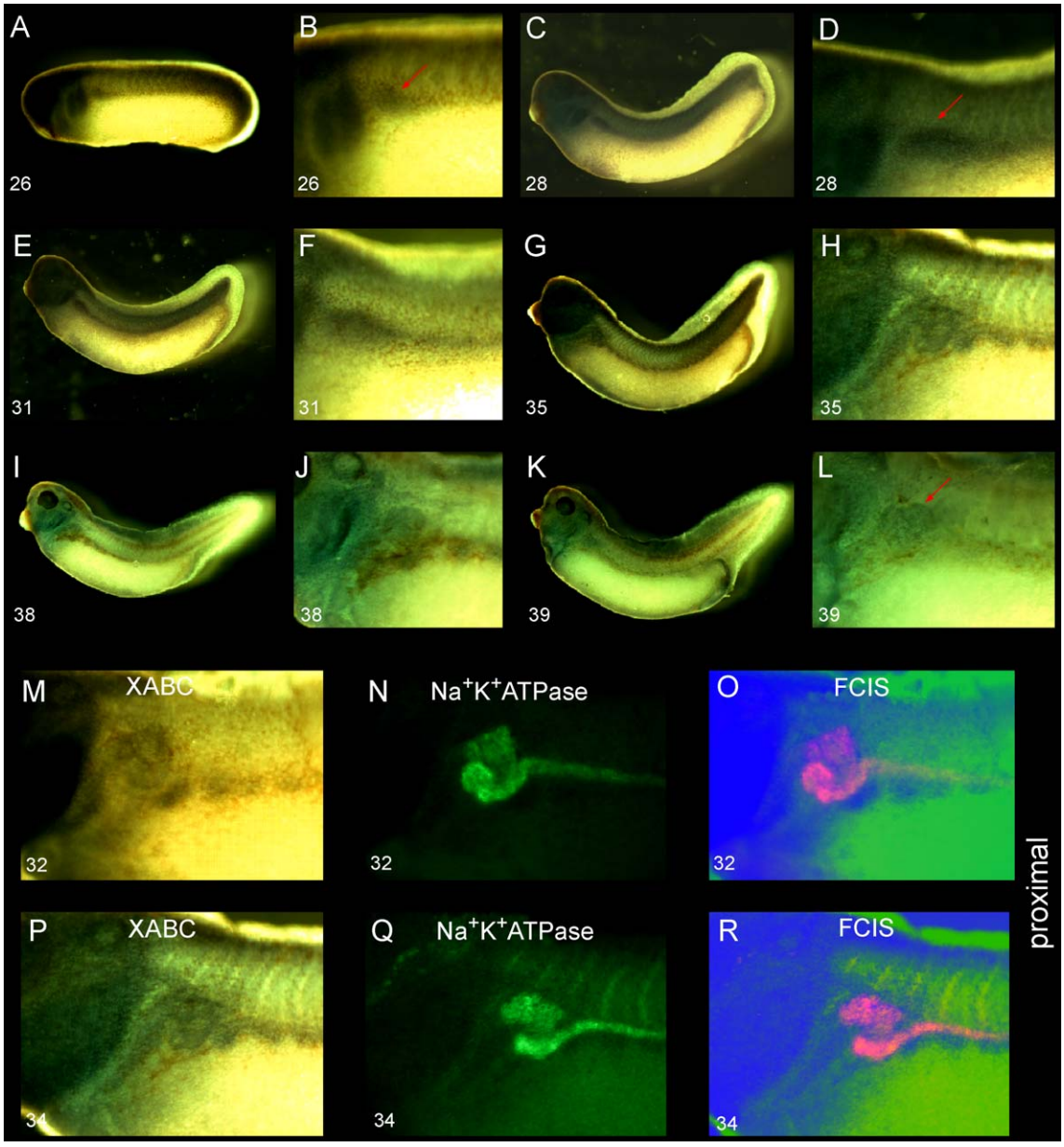

Fig. 6. Pronephric expression of an ABC transporter. Embryo stages are shown on the lower left of each panel. XABC expression in the pronephros is first detected at stage 26 (A and B), red arrow. The XABC1 gene is expressed in both early and late proximal segments (A–L). Other expressing tissues include the somites, brachial arches, and head. By stage 35, expression of XABC in nonpronephric tissues increases, necessitating shorter development times, hence the relatively weak signal in later panels. Panels M–R illustrates FCIS staining. Purple development of the transporter is shown in the left column, FITC-tyramide development of the Na^+K^+ATPase counterstain shown in the middle, and FCIS overlay shown on the right.

were found to be expressed at high levels in the pronephros, each of which is found in a unique pattern. XNBC1 is most similar to the widely studied salamander electrogenic sodium bicarbonate cotransporter (SLC4A4/NBC1, Romero et al., 1997) while XNBC2 is related to SLC4A11 (Parker et al., 2001; Table 2). In humans, SLC4A4 defects are associated with proximal tubule acidosis (Igarashi et al., 1999).

XNBC1 is expressed in two domains within the pronephros (Fig. 7). The first of these is a low-level expression domain in the early and late proximal tubule, which begins at stage 29; the second is high level expression in a unique domain that commences at stage 33 and marks the late portion of the distal segment. Once active expression in this distal domain is much higher than in the early proximal segment. This is the first pronephric marker reported for a late distal domain. Strong expression begins in the pronephros posterior to the bend that separates the pronephros from the pronephric duct. Weak expression in the early proximal tubule is maintained but becomes much less obvious than

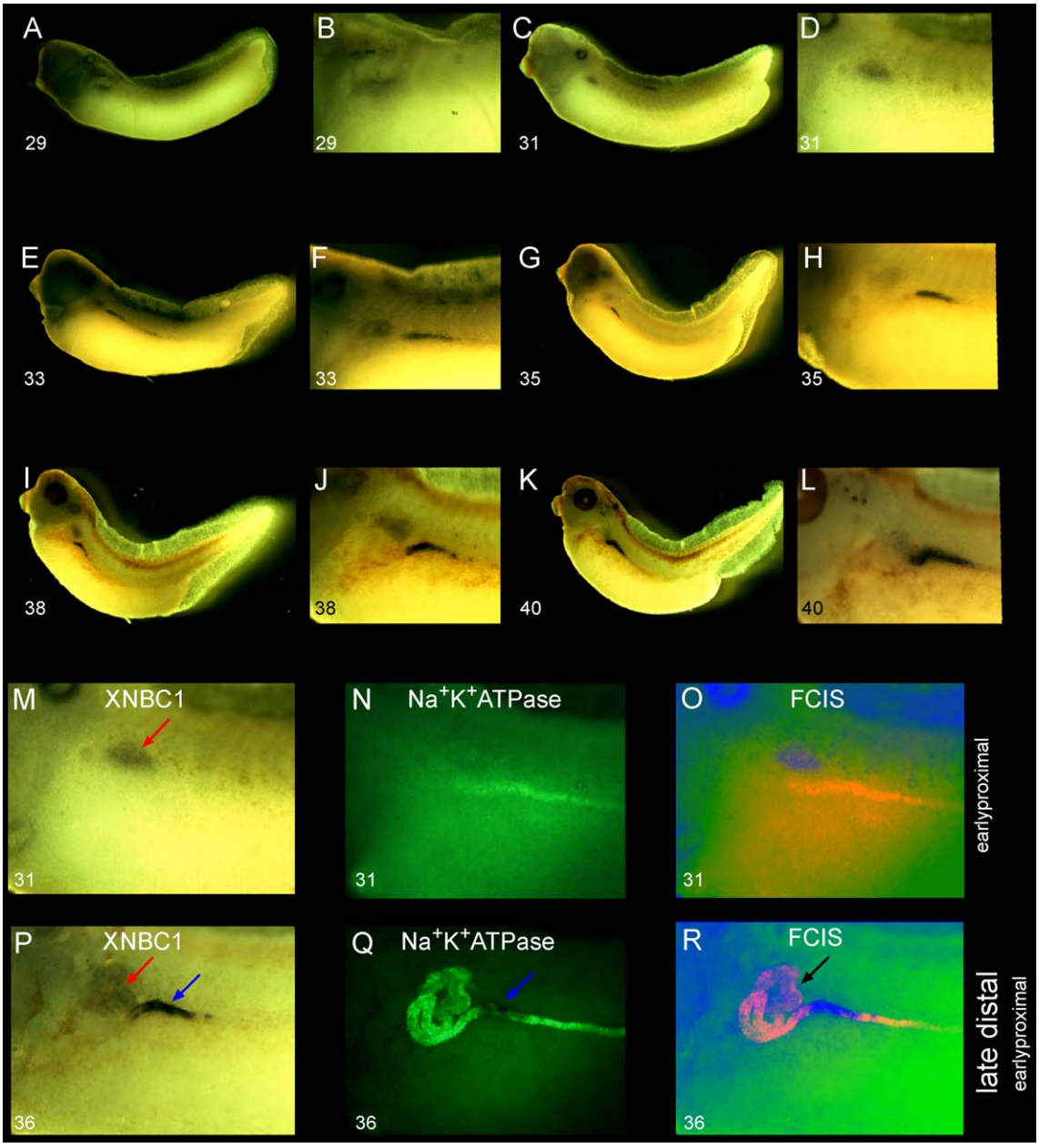

Fig. 7. XNBC1 expression in the developing kidney. XNBC1 is expressed in multiple pronephric regions. Expression in the early and late proximal domains begins at stage 29. At stage 33, a new domain of expression is activated in the late distal segment. Once active, this segment expresses much higher levels of XNBC1 than do the proximal tubules. Proximal expression declines over time and is barely detectable by stage 40, at which time late distal expression remains robust. Red arrow, proximal tubule expression. Blue arrow, late distal segment expression. Black arrow, pink coloration in proximal tubules representing low-level expression.

the strong expression in the late distal domain by stage 36 (see Figs. 7F, R).

XNBC2 is expressed in the early proximal domain from stage 26 onwards and also at lower levels in the early distal domain, but is absent or at much lower levels in the intervening late proximal domain (Fig. 8). This can be seen to different extents in various samples between stages 32 and 34. By stage 38, the early distal expression drops to very low levels and the only major site of pronephric transcription is the early proximal domain.

Kidney-specific Na-K-Cl cotransporter (NKCC2)

Defects in the renal Na-K-2Cl cotransporter NKCC2 are responsible for Bartter's syndrome in humans, an inherited hypokalaemic alkalosis (Simon et al., 1996). In mammals, this gene is expressed in the thick ascending limb and in the macula densa (Yang et al., 1996). In *Xenopus* pronephroi, XNKCC2 is strongly expressed in the early distal segment from stage 29 onwards (Fig. 9). It may also be expressed in a few cells in the proximal most portion of the late distal

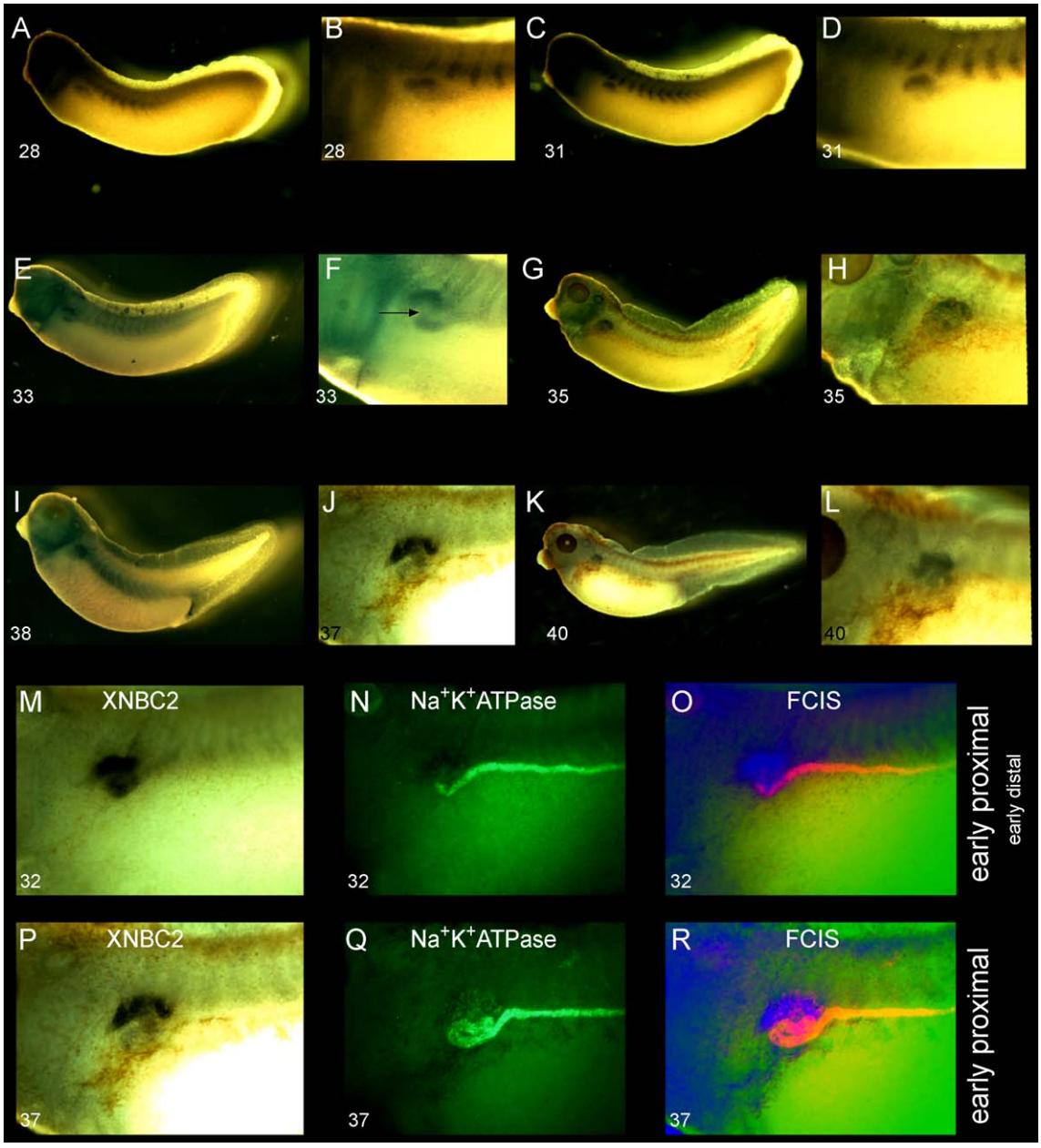

Fig. 8. XNBC2 expression. XNBC2 is expressed in the pronephros from stage 28. Up until stage 35, expression is present in both the early proximal and early distal segments, but at only very low levels in the intervening late proximal segment (see panel F, black arrow). The early distal expression decreases over time and cannot be detected by stage 35. From stage 35 onwards, strong expression is observed in the early proximal segment and the weak expression in the late proximal domain is also retained.

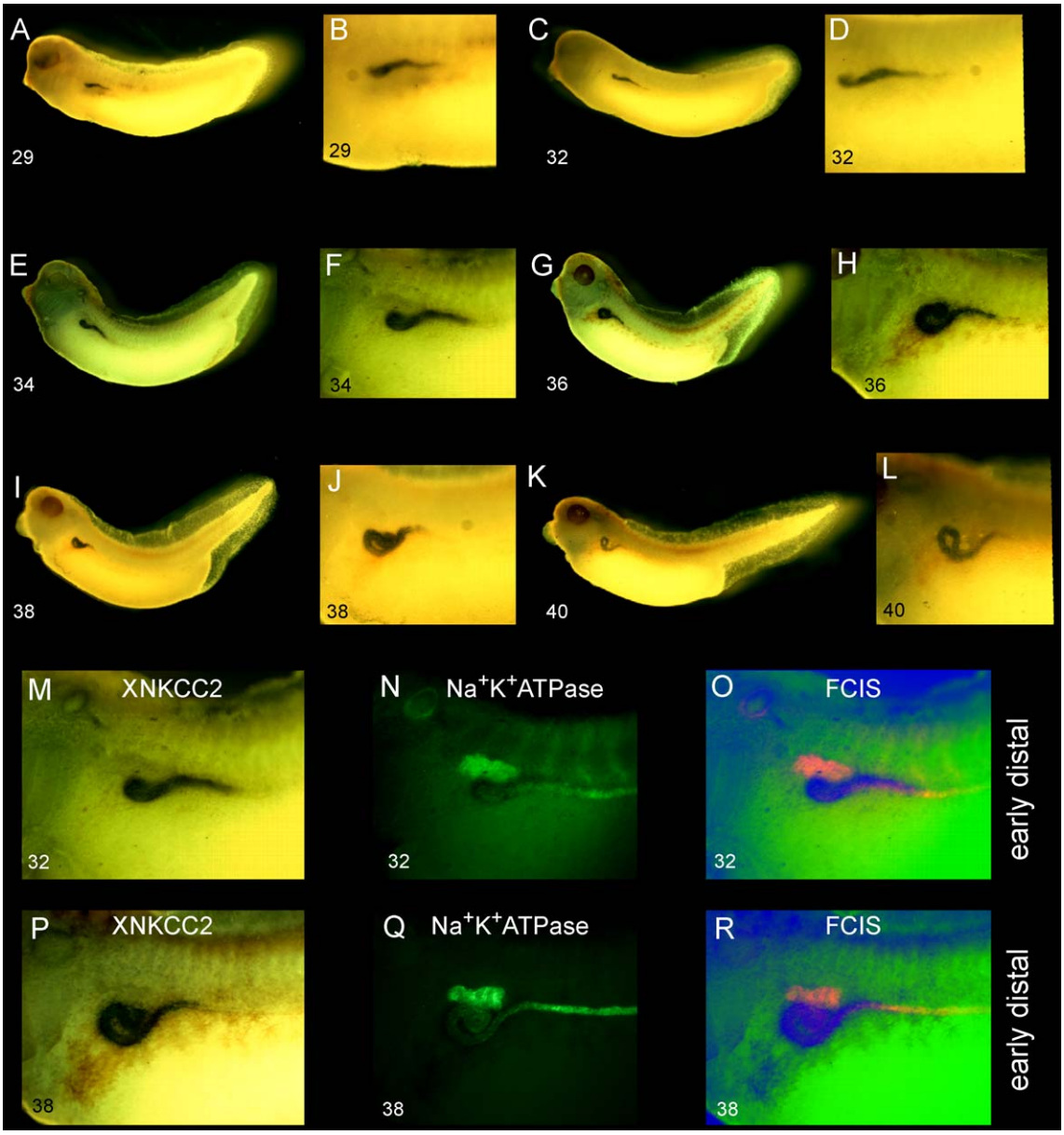

Fig. 9. XNKCC2 is a pronephric specific marker of the early distal segment. XNKCC2 expression is first detected at stage 29 when strong expression commences in the future early proximal segment. This pattern is maintained until at least stage 40.

segment. Expression in the early distal segment is similar to that of xClCk (Vize, 2003), but XNKCC2 is more convenient as a distal marker, as xClCk is also expressed in the late distal segment and pronephric duct—albeit at lower levels.

Stress-induced organic solute cotransporter (ROSIT)

XROSIT (Table 2) is most closely related to a rat protein that encodes a Na^+- and Cl^--dependent organic solute cotransporter that is induced in response to hypertonic stress (Wasserman et al., 1994). Related cotransporters have been identified for neurotransmitters, amino acids, and organic osmolytes. The *Xenopus* XROSIT gene is expressed in early proximal tubules at high levels and at low levels in the late proximal domain (Fig. 10). Expression begins in the pronephros at stage 27/28.

Zinc transporter (SLC30A1)

Zinc transporters facilitate zinc movement across cellular and intracellular membranes, and mutations in murine SLC30A1 are embryonic lethal (Palmiter and Huang, 2004). XZnSLC30 shows strong expression in the most extreme proximal tips of the dorsal branches from NF stage 28 onwards (Fig. 11). By stage 35, expression is a little more widespread in the early proximal segment, but remains focused at the dorsal branch tips. Other genes have been

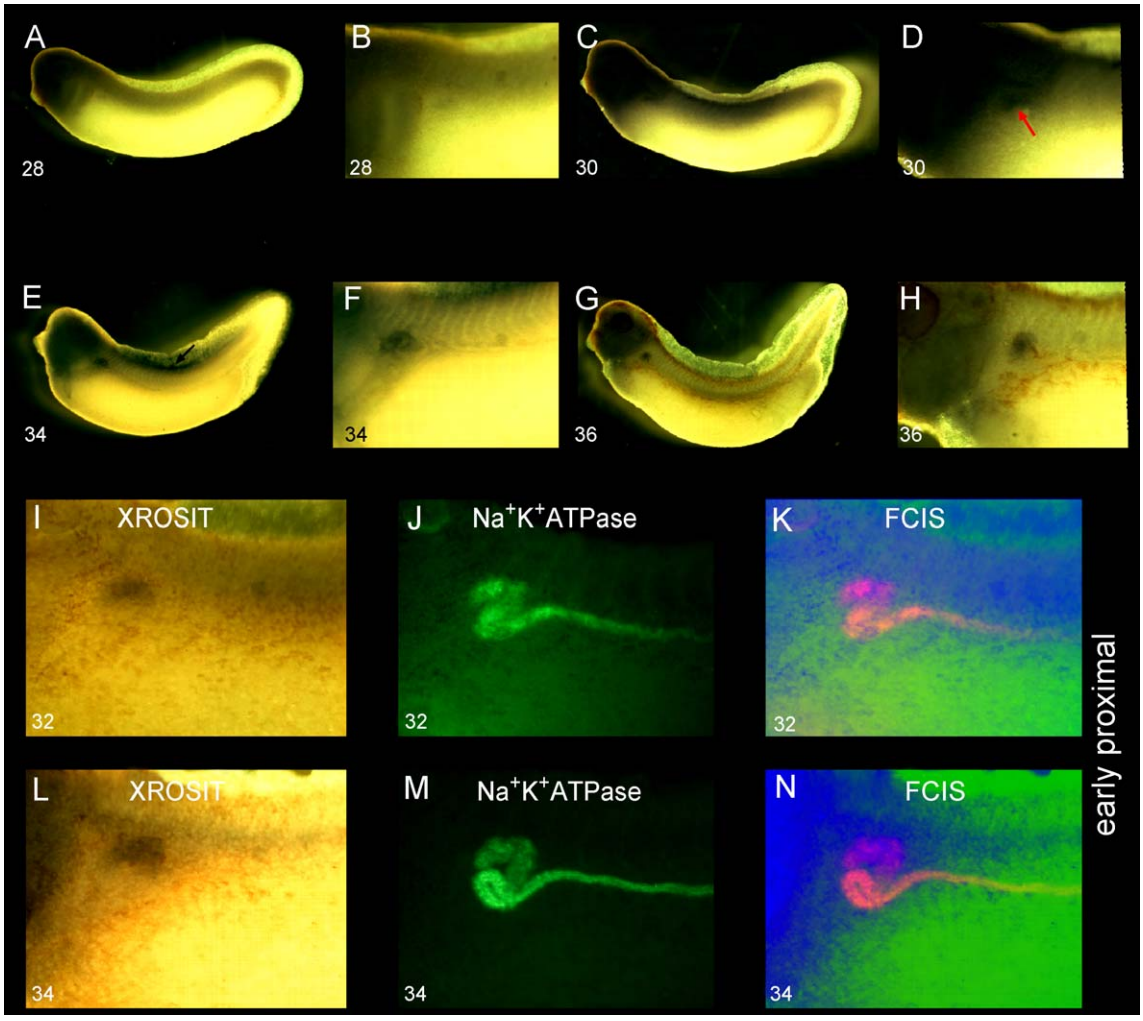

Fig. 10. Expression of XROSIT, an organic solute cotransporter. XROSIT is expressed in a small pronephric domain from stage 28 onwards. Staining in the dorsal fin (black arrow, panel E) is background and was also observed in controls. In conventional staining (panels A–H), precise localization within the pronephros is difficult, but the FCIS overlap (panel K) clearly shows that expression is restricted to the early proximal domain (pink region, panel K).

reported to be expressed in the dorsal branches, most notably transcription factors involved in kidney specification (Carroll and Vize, 1999), but this is the first transporter to be found expressed in such a pattern.

Discussion

The pronephros is a powerful system in which to apply experimental embryology to the analysis of kidney organogenesis. The question of how physiologically similar the pronephros is to mammalian nephrons therefore bears upon the distinction between pronephroi being a quaint model system and the potential for pronephric studies to lead to insights into the process of kidney organogenesis in general. Gene interactions first identified in pronephroi (Carroll and Vize, 1999) have subsequently been found to hold true in mammals (Bouchard et al., 2002), but how similar the two organs are in terms of physiological function has not previously been addressed in detail. In the present study, the localization of transport processes and transporter gene expression was mapped in pronephroi. The results identify multiple distinct domains within pronephric tubules and imply a complexity of function on par with that of nephrons within adult mammalian kidneys. They also provide sensitive and powerful markers with which proximo-distal patterning can now be examined.

Pronephric segments

Mesonephric nephrons have been classified as having a single proximal domain (Gérard and Cordier, 1934a,b; Møbjerg et al., 1998; Yucha and Stoner, 1986). Metanephroi, the adult kidneys of mammals, have a proximal segment that can be subdivided into a convoluted segment and a straight segment—the former may correspond to the pronephric early proximal segment and the latter to the pronephric late proximal segment. The mammalian convoluted

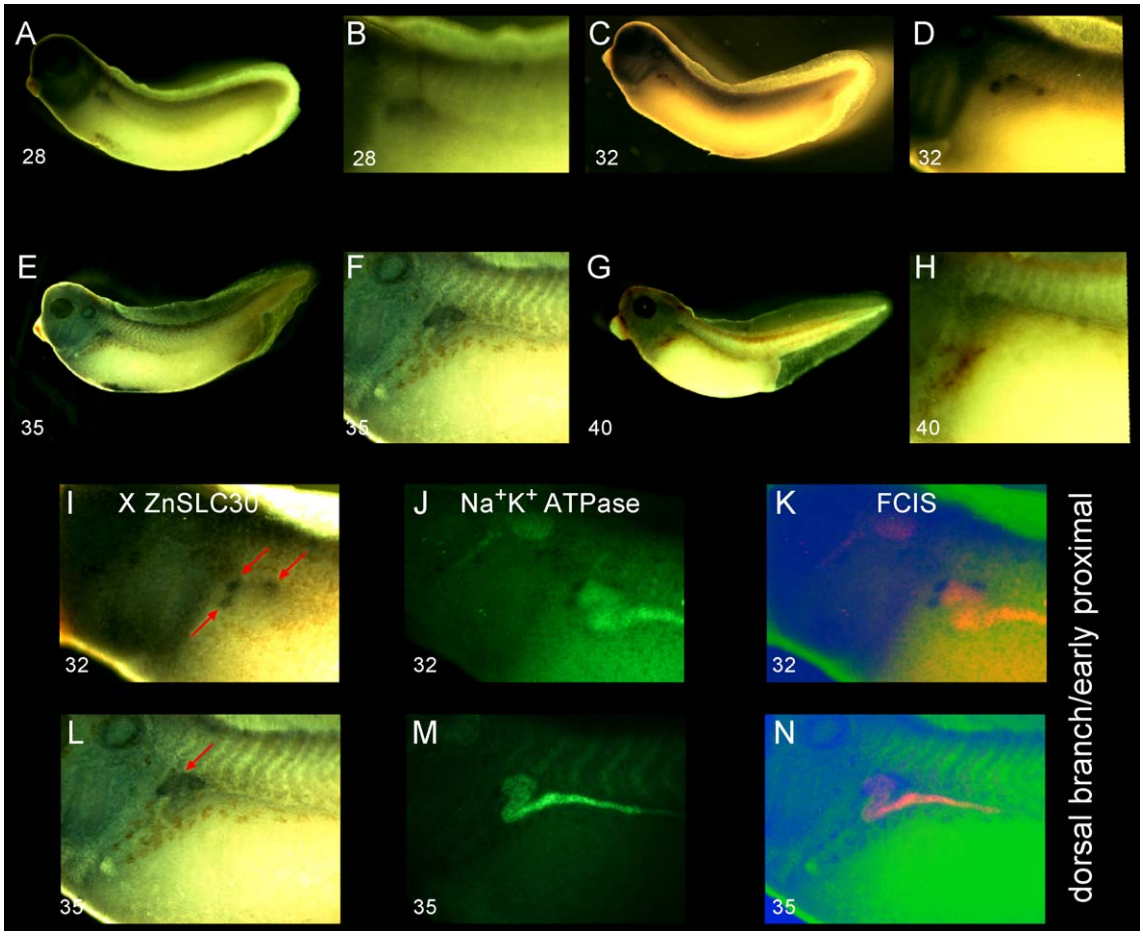

Fig. 11. Expression of a zinc transporter, XZnSLC30, in the embryonic kidney tubules. XZnSLC30 (M–R) is expressed in the tips of the dorsal branches at commencing at stage 28. By stage 35, this expression has expanded slightly into the early proximal segment (panels F and N) but expression remains highest in the dorsal branches. As the pronephric tubules coil, the staining is still present but is less obvious as the dorsal branches lie proximal to the lateral coiled tubules (H).

proximal segment can be further subdivided into S1 and S2 domains, and the proximal straight segment is called the S3 segment. Mammalian proximal segments differ from each other in terms of both transport processes and cell ultrastructure (Dantzler, 1988; O'Callaghan and Brenner, 2000). The proximal tubules of frog pronephroi have a brush border like that of mammalian proximal segments (Kluge and Fischer, 1991; Møbjerg et al., 2000; Vize et al., 1995, 2003a). Data presented in this report demonstrates that this region can be subdivided into three domains based on the expression of cotransporters: the dorsal branches, the early proximal tubule, and the late proximal tubule. In pronephroi, the dorsal branches express XZnSLC30, the early proximal segment is best detected with XAA2 (Fig. 5) or XNBC2 (Fig. 8), and the late proximal segment with XAA1 (Fig. 4). The proximal tubule is the major site of amino acid recovery in mammalian nephrons (Silbernagl, 1988), consistent with the localization of XAA1 and XAA2. In mammals, the closest known homologues of XAA1 and XAA2 are also expressed in the proximal segments, but their precise localization has not yet been reported (Avissar et al., 2001; Fernandez et al., 2003). The mammalian SLC30 zinc transporter is, like its *Xenopus* orthologue, expressed in the convoluted proximal segment (Ranaldi et al., 2002), analogous to the early proximal segment of the pronephros.

Mesonephric kidneys have a distal domain that can be functionally subdivided into an early (or diluting) segment and a late distal tubule (Møbjerg et al., 1998; Yucha and Stoner, 1986). The mesonephric late distal segment participates in acid secretion (Stanton et al., 1987) and bicarbonate resorption (Yucha and Stoner, 1986). The *Xenopus* pronephric distal nephron has at least two subdomains demarcated by expression of XNKCC2 in the early domain and XNBC1 in the late domain. The NKCC2 cotransporter that plays a key role in the thick ascending limb of mammals where it generates an electrochemical gradient is in turn used to drive transport of many other ions such as calcium, magnesium, and sodium (O'Callaghan and Brenner, 2000). The presence of high levels of XNKCC2 in the frog early distal domain implies similar mechanisms may function in the pronephros. The frog distal nephron is very important for ion resorption in mesonephroi; for example it, is the

major site of sodium resorption (Dantzler, 1988) and NKCC2 may play a key role in driving such processes. Mutations in NKCC2 cause Bartter's syndrome in humans (Simon et al., 1996) and pronephroi may be a useful model in which to study the function of this gene.

The late distal domain identified by expression of XNBC1 may correspond to the site of bicarbonate production associated with acidification of urine. In the salamander, late distal segment bicarbonate resorption is dependent on carbonic anhydrase and lumenal sodium (Yucha and Stoner, 1986). Previous studies of NBC1 in salamander kidneys were found anti-NBC immunoreactivity in both the proximal and distal segments (Maunsbach et al., 2000), but differences in the level of expression similar to those shown in Fig. 5 were not reported. Bicarbonate transport occurs in both segments, but transport is much higher in the distal region (Yucha and Stoner, 1986), the site of XNBC1 transcription. In mammals, NBC1 is expressed in the S1 and S2 segments of the proximal tubule (Maunsbach et al., 2000). The expression pattern of mammalian NBC2/SLC4A11 (Parker et al., 2001) has not yet been described. Fig. 12 presents a summary of the localized expression of transporters in the *Xenopus* pronephric nephron compared to known expression patterns within mammalian metanephric nephrons.

Pronephric resorption of macromolecules

The glomerular filter barrier of mammalian nephrons allows molecules with a diameter of 1.4 nm to cross freely, while proteins such as albumin (3.6 nm) cross at much lower rates (Kanwar et al., 1991). Some albumin manages to cross the filter barrier in humans, but is effectively recovered via megalin- and cubulin-dependent endocytosis (reviewed by Christensen and Birn, 2002; Gekle, 1998). The ultrastructural features of the filtration barrier are the same in glomera and glomeruli (Drummond, 2000; Drummond et al., 1998a), with pronephroi possessing a glomeral basement membrane and podocytes (Kluge and Fischer, 1990). The labeling of urine in *Xenopus* embryos from circulating fluorescent proteins indicates that despite expectations, considerable glomeral macromolecule filtration is occurring. Over 90% of kidneys filter dextrans into the kidney tubule lumen, but only 54% of tadpole kidneys leak serum albumin (Table 1). This indicates that for serum proteins, the filtration barrier effectively limits passage in the remaining 46% of glomera. Variable degrees of pronephric epithelial labeling are also observed in tadpoles with circulating fluorescent serum albumin, with some displaying only a small fraction of the labeling observed in others. In some pronephric kidneys, resorption is sufficient for most of the fluor to be present in the epithelia, with little or none remaining in the lumen of the kidney. In others, there is no pronephric fluorescence at all indicating that the glomeral filtration barrier has effectively blocked the passage of the protein. As the protein leakage rate for BSA is 54%, experimental interventions that damage the *Xenopus* glomeral filtration properties would presumably lead to an increase in the number of glomera showing protein filtration and allow proteinuria to be assayed in this system. Interventions that improved protein retention, either genetic or pharmaceutical, would decrease the number from 54% toward zero.

Given that protein loss caused by glomerular barrier breakdown is fatal in humans, the filtration of proteins observed in pronephroi may reflect the immature nature of the forming glomus. We are currently investigating this possibility. The filtration of macromolecules described here

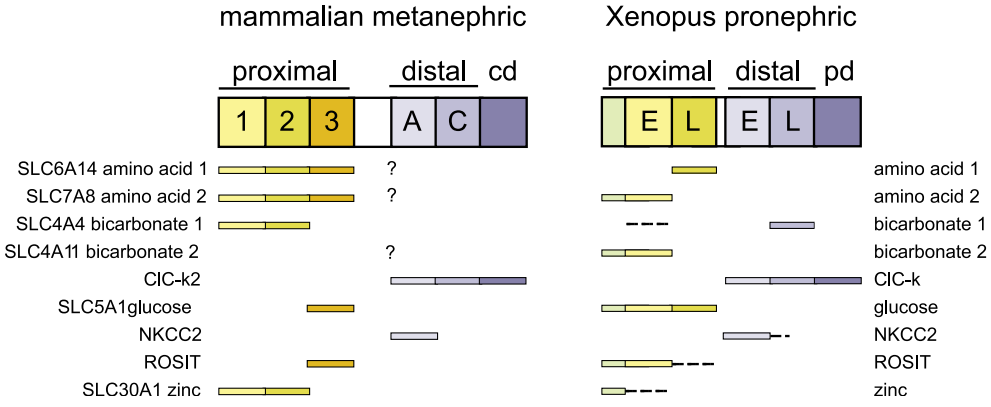

Fig. 12. Expression of transporters in mammalian metanephric and *Xenopus* pronephric nephrons. Mammalian metanephric nephrons have a proximal domain subdivided into three segments: S1 (1), S2 (2) and S3 (3). S1 and S2 are also known as the proximal convoluted segments and S3 as the proximal straight segment. S3 is followed by the loop of Henle (LH), or thin loop. The distal segment is comprised of the thick ascending limb (A) (also known as the distal straight segment) and the convoluted distal segment (C), which is followed by the collecting duct (cd). Pronephric proximal and distal domains both have an early (E) and a late (L) segment, and are sometimes separated by a short ciliated intermediate segment. The localization of *Xenopus* transporters is shown below the corresponding segments. The localization of the closest known mammalian gene is also shown. As some of these transporters belong to very large families, it is possible that some of these genes are not orthologues. Mammalian localization references are SLC6A14, Avissar et al. (2001); SLC7A8, Fernandez et al. (2003); SLC4A4, Maunsbach et al. (2000); SLC4A11, no information; ClC-k2, Adachi et al. (1994); SLC5A1, You et al. (1995); NKCC2, Lee et al. (1994), Payne and Forbush (1994); ROSIT, Obermuller et al. (1997); SLC30A1, Ranaldi et al. (2002); XClCk, Vize et al. (2003a).

can be visualized in living *Xenopus* tadpoles using a simple fluorescence stereoscope. Similar processes have also been visualized in live rodents, but this requires the use of a two-photon confocal microscope and vastly more complicated animal handling (Dunn et al., 2002).

The data presented in this report establish that pronephric nephrons display a level of proximo-distal transport specialization on par with that of human nephrons. In fact, the massive rate of urine production (see BSA_proteinuria.mov, supplemental materials) and potential for solute loss in an aqueous environment probably requires pronephroi to be especially effective at recovery processes. Macromolecules are resorbed in the proximal segment, which also expresses cotransporters for recovery of amino acids, bicarbonate, glucose, sodium, and zinc. The early pronephric distal segment expresses high levels of the NKCC2 cotransporter and the late distal segment expresses high levels of a sodium bicarbonate cotransporter, possibly indicating bicarbonate recovery as a byproduct of urine acidification. The *Xenopus* pronephric kidney is therefore a useful system for investigating a wide variety of physiological processes.

Acknowledgments

Development of the Photoshop processing methods described here was performed by Victor Gerth, who also helped with videography. Renal uptake assay injections were performed by Anna Urban and Scott Livingstone. I would like to thank Paul Gordon, Christoph Sensen, and Jeff Bowes for help with the MAGPIE analysis and general bioinformatics assistance. Teri Jo Mauch and Lance Davidson provided invaluable feedback and FISH protocols. This work was supported by grants from the NSF (IBN 9983061), CIHR and Alberta Heritage Fund for Medical Research and PDV is a Senior Scholar of the AHFMR.

References

Adachi, S., Uchida, S., Ito, H., Hata, M., Hiroe, M., Marumo, F., Sasaki, S., 1994. Two isoforms of a chloride channel predominantly expressed in thick ascending limb of Henle's loop and collecting ducts of rat kidney. J. Biol. Chem. 269, 17677–17683.

Avissar, N.E., Ryan, C.K., Ganapathy, V., Sax, H.C., 2001. Na^+-dependent neutral amino acid transporter ATB0 is a rabbit epithelial cell brush-border protein. Am. J. Physiol: Cell Physiol. 281, C963–C971.

Balinsky, J.B., 1970. Nitrogen metabolism in amphibians. In: Campbell, J.W. (Ed.), Comparative Biochemistry of Nitrogen MetabolismThe Vertebrates, vol. 2. Academic Press, London, pp. 519–637.

Biemesderfer, D., Stanton, B., Wade, J.B., Kashgarian, M., Giebisch, G., 1989. Ultrastructure of *Amphiuma* distal nephron: evidence for cellular heterogeneity. Am. J. Physiol. 256, C849–C857.

Bouchard, M., Souabni, A., Mandler, M., Neubuser, A., Busslinger, M., 2002. Nephric lineage specification by Pax2 and Pax8. Genes Dev. 16, 2958–2970.

Carroll, T.J., Vize, P.D., 1999. Synergism between Pax-8 and lim-1 in embryonic kidney development. Dev. Biol. 214, 46–59.

Christensen, E.I., Birn, H., 2002. Megalin and cubilin multifunctional endocytic receptors. Nat. Rev. Mol. Cell Biol. 3, 256–266.

Dantzler, W.H., 1988. Comparative Physiology of the Vertebrate Kidney. Springer-Verlag, Berlin.

Davidson, L.A., Keller, R.E., 1999. Neural tube closure in *Xenopus laevis* involves medial migration, directed protrusive activity, cell intercalation and convergent extension. Development 126, 4547–4556.

Drummond, I.A., 2000. The zebrafish pronephros: a genetic system for studies of kidney development. Pediatr. Nephrol. 14, 428–435.

Drummond, I.A., Majumdar, A., Hentschel, H., Elger, M., Solnica-Krezel, L., Schier, A.F., Neuhauss, S.C., Stemple, D.L., Zwartkruis, F., Rangini, Z., Driever, W., Fishman, M.C., 1998a. Early development of the zebrafish pronephros and analysis of mutations affecting pronephric function. Development 125, 4655–4667.

Drummond, I.A., Majumdar, A., Hentschel, H., Elger, M., Solnica-Krezel, L., Schier, A.F., Neuhauss, S.C., Stemple, D.L., Zwartkruis, F., Rangini, Z., Driever, W., Fishman, M.C., 1998b. Early development of the zebrafish pronephros and analysis of mutations affecting pronephric function. Development 125, 4655–4667.

DuBose, T.D., 1990. Reclamation of filtered bicarbonate. Kidney Int. 38, 584–589.

Dunn, K.W., Sandoval, R.M., Kelly, K.J., Dagher, P.C., Tanner, G.A., Atkinson, S.J., Bacallao, R.L., Molitoris, B.A., 2002. Functional studies of the kidney of living animals using multicolor two-photon microscopy. Am. J. Cell Physiol. 283, C905–C916.

Eid, S.R., Brandli, A.W., 2001. *Xenopus* Na,K-ATPase: primary sequence of the beta2 subunit and in situ localization of alpha1, beta1, and gamma expression during pronephric kidney development. Differentiation 68, 115–125.

Eid, S.R., Terrettaz, A., Nagata, K., Brandli, A.W., 2002. Embryonic expression of *Xenopus* SGLT-1L, a novel member of the solute carrier family 5 (SLC5), is confined to tubules of the pronephric kidney. Int. J. Dev. Biol. 46, 177–184.

Fernandez, E., Torrents, D., Chillaron, J., Martin Del Rio, R., Zorzano, A., Palacin, M., 2003. Basolateral LAT-2 has a major role in the transepithelial flux of Lcystine in the renal proximal tubule cell line OK. J. Am. Soc. Nephrol. 14, 837–847.

Fox, H., 1963. The amphibian pronephros. Q. Rev. Biol. 38, 1–25.

Gekle, M., 1998. Renal proximal tubular albumin reabsorption: daily prevention of albuminuria. News Physiol. Sci. 13, 5–11.

Gérard, P., Cordier, R., 1934a. Esquisse d'une histopathologie compaže du rein des vertebrates. Biol. Rev. Cambridge Philos. Soc. 9, 110–131.

Gérard, P., Cordier, R., 1934b. Recherches d'histophysiologie compaže sur le pro–et le mžesonžephros larvaires des anoures. Z. Zellforsch. Mikrosk. Anat. 21, 1–23.

Goodrich, E.S., 1930. Studies on the Structure and Development of Vertebrates. Macmillan and Co., London.

Harland, R.M., 1991. In situ hybridization: an improved whole-mount method for *Xenopus* embryos. Methods Cell Biol. 36, 685–695.

Hediger, M.A., Coady, M.J., Ikeda, T.S., Wright, E.M., 1987. Expression cloning and cDNA sequencing of the Na+/glucose co-transporter. Nature 330, 379–381.

Igarashi, T., Inatomi, J., Sekine, T., Cha, S.H., Kanai, Y., Kunimi, M., Tsukamoto, K., Satoh, H., Shimadzu, M., Tozawa, F., Mori, T., Shiobara, M., Seki, G., Endou, H., 1999. Mutations in SLC4A4 cause permanent isolated proximal renal tubular acidosis with ocular abnormalities. Nat. Genet. 23, 264–266.

Kanwar, Y.S., Liu, Z., Kashihara, N., Wallner, E.I., 1991. Current status of the structural and functional basis of glomerular filtration and proteinuria. Semin. Nephrol. 11, 390–413.

Kekuda, R., Prasad, P.D., Fei, Y.J., Torres-Zamorano, V., Sinha, S., Yangfeng, T.L., Leibach, F.H., Ganapathy, V., 1996. Cloning of the sodium-dependent, broad-scope, neutral amino acid transporter BO from a human placental choriocarcinoma cell line. J. Biol. Chem. 271, 18657–18661.

Kluge, B., Fischer, A., 1990. The pronephros of the early ammocoete larva of lampreys: fine structure of the external glomus. Cell Tissue Res. 260, 249–259.

Kluge, B., Fischer, A., 1991. The pronephros of the early ammocoete larva of lampreys: fine structure of the renal tubules. Cell Tissue Res. 263, 515–528.

Lee, I., Hediger, M.A., Hebert, S.C., 1994. Molecular cloning, primary structure, and characterization of two members of the mammalian electroneutral sodium (potassium)-chloride cotransporter family expressed in kidney. J. Biol. Chem. 269, 17713–17722.

Lencer, W.I., Weyer, P., Verkman, A.S., Ausiello, D.A., Brown, D., 1990. FITC-dextran as a probe for endosome function and localization in kidney. Am. J. Physiol. 258, C309–C317.

Levine, A.J., Munoz-Sanjuan, I., Bell, E., North, A.J., Brivanlou, A.H., 2003. Fluorescent labeling of endothelial cells allows in vivo, continuous characterization of the vascular development of *Xenopus laevis*. Dev. Biol. 254, 50–67.

Martin, M.G., Turk, E., Lostao, M.P., Kerner, C., Wright, E.M., 1996. Defects in Na+/glucose cotransporter (SGLT1) trafficking and function cause glucose–galactose malabsorption. Nat. Genet. 12, 216–220.

Maunsbach, A.B., Vorum, H., Kwon, T.H., Nielsen, S., Simonsen, B., Choi, I., Schmitt, B.M., Boron, W.F., Aalkjaer, C., 2000. Immunoelectron microscopic localization of the electrogenic Na/HCO(3) cotransporter in rat and ambystoma kidney. J. Am. Soc. Nephrol. 11, 2179–2189.

Møbjerg, N., Larsen, E.H., Jesperson, A., 1998. Morphology of the nephron in the mesonephros of *Bufo bufo* (Amphibia, Anura, Bufonidae). Acta Zool. 79, 31–50.

Møbjerg, N., Larsen, E.H., Jesperson, A., 2000. Morphology of the kidney in larvae of *Bufo viridis*. J. Morphol. 245, 177–195.

Nagata, K., Hori, N., Sato, K., Ohta, K., Tanaka, H., Hiji, Y., 1999. Cloning and functional expression of an SGLT-1-like protein from the *Xenopus laevis* intestine. Am. J. Physiol. 276, G1251–G1259.

Nieuwkoop, P.D., Faber, J., 1994. Normal Table of *Xenopus Laevis* (Daudin). Garland, New York.

Obermuller, N., Kranzlin, B., Verma, R., Gretz, N., Kriz, W., Witzgall, R., 1997. Renal osmotic stress-induced cotransporter: expression in the newborn, adult and post-ischemic rat kidney. Kidney Int. 52, 1584–1592.

O'Callaghan, C.A., Brenner, B.M., 2000. The Kidney at a Glance. Blackwell, Oxford.

Palmiter, R.D., Huang, L., 2004. Efflux and compartmentalization of zinc by members of the SLC30 family of solute carriers. Pflugers Arch. 447, 744–751.

Parker, M.D., Ourmozdi, E.P., Tanner, M.J., 2001. Human BTR1, a new bicarbonate transporter superfamily member and human AE4 from kidney. Biochem. Biophys. Res. Comm. 282, 1103–1109.

Payne, J.A., Forbush, B., 1994. Alternatively spliced isoforms of the putative renal Na-K-Cl cotransporter are differentially distributed within the rabbit kidney. Proc. Natl. Acad. Sci. U. S. A. 91, 4544–4548.

Ranaldi, G., Perozzi, G., Truong-tran, A., Zalewski, P., Murgia, C., 2002. Intracellular distribution of labile Zn(II) and zinc transporter expression in kidney and MDCK cells. Am. J. Physiol.: Renal. Physiol. 283, F1365–F1375.

Richards, A.N., 1929. Methods and Results of Direct Investigations of the Function of the Kidney. Williams and Wilkins Company, Baltimore.

Romero, M.F., Hediger, M.A., Boulpaep, E.L., Boron, W.F., 1997. Expression cloning and characterization of a renal electrogenic Na+/HCO3− cotransporter. Nature 387, 409–413.

Satlin, L.M., Woda, C.B., Schwartz, G.J., 2003. Development of function in the metanephric kidney. In: Vize, P.D., Woolf, A.S., Bard, J.B. (Eds.), The Kidney: From Normal Development to Congenital Disease. Academic Press, Amsterdam; p. 278–325.

Silbernagl, S., 1988. The renal handling of amino acids and oligopeptides. Physiol. Rev. 68, 911–1007.

Simon, D.B., Karet, F.E., Hamdan, J.M., DiPietro, A., Sanjad, S.A., Lifton, R.P., 1996. Bartter's syndrome, hypokalaemic alkalosis with hypercalciuria, is caused by mutations in the Na-K-2Cl cotransporter NKCC2. Nat. Genet. 13, 183–188.

Sive, H.L., Grainger, R.M., Harland, R.M., 2000. Early Development of *Xenopus Laevis*. Cold Spring Harbor Laboratory Press, Cold Spring Harbor.

Stanton, B., Biemesderfer, D., Stetson, D., Kashgarian, M., Giebisch, G., 1984. Cellular ultrastructure of *Amphiuma* distal nephron: effects of exposure to potassium. Am. J. Physiol. 247, C204–C216.

Stanton, B., Omerovic, A., Koeppen, B., Giebisch, G., 1987. Electroneutral H+ secretion in distal tubule of *Amphiuma*. Am. J. Physiol. 252, F691–F699.

Torrents, D., Estevez, R., Pineda, M., Fernandez, E., Lloberas, J., Shi, Y., Zorzano, A., Palacin, M., 1998. Identification and characterization of a membrane protein (y+L amino acid transporter-1) that associates with 4F2hc to encode the amino acid transport activity y+L—a candidate gene for lysinuric protein intolerance. J. Biol. Chem. 273, 32437–32445.

Uochi, T., Takahashi, S., Ninomiya, H., Fukui, A., Asashima, M., 1997. The Na+, K+-ATPase alpha subunit requires gastrulation in the *Xenopus* embryo. Dev. Growth Differ. 39, 571–580.

Vize, P.D., 2003. The chloride conductance channel ClC-K is a specific marker for the *Xenopus* pronephric distal tubule and duct. Gene. Exp. Patterns 3, 347–350.

Vize, P.D., Jones, E.A., Pfister, R., 1995. Development of the *Xenopus* pronephric system. Dev. Biol. 171, 531–540.

Vize, P.D., Carroll, T.J., Wallingford, J.B., 2003a. Induction, development and physiology of the pronephric tubules. In: Vize, P.D., Woolf, A.S., Bard, J.B.L. (Eds.), The Kidney: From Normal Development to Congenital Disease. Academic Press, Amsterdam; p. 19–50.

Vize, P.D., Woolf, A.S., Bard, J.B.L., 2003b. The Kidney: From Normal Development to Congenital Disease. Academic Press, Amsterdam.

Wasserman, J.C., Delpire, E., Tonidandel, W., Kojima, R., Gullans, S.R., 1994. Molecular characterization of ROSIT, a renal osmotic stress-induced Na(+)–Cl (−)-organic solute cotransporter. Am. J. Physiol. 267, F688–F694.

Wood, I.S., Trayhurn, P., 2003. Glucose transporters (GLUT and SGLT): expanded families of sugar transport proteins. Br. J. Nutr. 89, 3–9.

Wright, E.M., Turk, E., 2004. The sodium/glucose cotransport family. Pflugers Arch. 447, 510–518.

Yang, T., Huang, Y.G., Singh, I., Schnermann, J., Briggs, J.P., 1996. Localization of bumetanide- and thiazide-sensitive Na-K-Cl cotransporters along the rat nephron. Am. J. Physiol. 271, F931–F939.

Ye, Z., Connor, J.R., 2000. cDNA cloning by amplification of circularized first strand cDNAs reveals non-IRE-regulated iron-responsive mRNAs. Biochem. Biophys. Res. Commun. 275, 223–227.

You, G., Lee, W.S., Barros, E.J., Kanai, Y., Huo, T.L., Khawaja, S., Wellsi, R.G., Nigam, S.K., Hediger, M.A., 1995. Molecular characteristics of Na1-coupled glucose transporters in adult and embryonic rat kidney. J. Biol. Chem. 270, 29365–29371.

Yucha, C.B., Stoner, L.C., 1986. Bicarbonate transport by amphibian nephron. Am. J. Physiol. 251, F865–F872.